Application of transient-time correlation functions to nonequilibrium molecular-dynamics simulations of elongational flow

B. D. Todd
Cooperative Research Centre for Polymers, CSIRO Division of Molecular Science, Private Bag 10, Clayton South MDC, Victoria 3169, Australia
(Received 21 May 1997)

The transient-time correlation function (TTCF) technique of Morriss and Evans [Mol. Phys. **54**, 629 (1985); Phys. Rev. A **35**, 792 (1987); Mol. Phys. **61**, 1151 (1987); Phys. Rev. A **38**, 4142 (1988); *Statistical Mechanics of Nonequilibrium Liquids* (Academic, London, 1990)] is applied to the case of an atomic fluid undergoing steady isothermal elongational flow. It is found that nonequilibrium molecular-dynamics TTCF calculations of the diagonal elements of the pressure tensor are extremely efficient for small applied strain rates, where the signal-to-noise ratio for the equivalent direct time-averaged pressures is far too low. At higher strain rates, TTCF is seen to faithfully reproduce the long-time steady-state values of the pressures, but is unable to account for observed transient oscillations. The technique thus provides an unambiguous means of calculating the long-time steady-state response of a fluid under steady elongational flow and opens the possibility of studying more complex molecular fluids under relatively weak flow, allowing for greater simulation time compared to the relaxation time of the fluid. [S1063-651X(97)01312-3]

PACS number(s): 61.20.Ja, 05.20.−y, 66.20.+d, 83.50.Jf

I. INTRODUCTION

Nonequilibrium molecular-dynamics (NEMD) simulations of elongational flow have been attempted by only a few groups over the past decade [1–6]. They are of significant interest because of the importance that rheological properties of fluids play in a number of chemical and manufacturing processes in the oil and polymer industries, for example. Elongational flow occurs when a fluid is stretched in at least one direction and compressed in at least another. However, the main technical difficulty in these types of simulations is the finite lifetime of a simulation due to the decrease of at least one of the simulation cell dimensions [1–5]. Eventually the simulation must cease, when the size of the cell in the contraction dimension reaches its minimum extension of twice the range of the interaction potential. The fluid must achieve a steady state well before this minimum extension is reached for a reliable estimate of the steady-state elongational viscosity to be made. For a simple atomic fluid, this is not a serious problem, for in general the relaxation time of the fluid is sufficiently smaller than the total simulation time. However, for complex molecular fluids the relaxation time may be significantly larger than the simulation time allowable, rendering any NEMD simulation of steady-state properties futile.

Recently, Todd and Daivis [6] devised a NEMD method that applies an oscillating strain rate to the equations of motion for a simple atomic fluid. This ensures that the system attains a temporally periodic steady state. For a given magnitude of the strain rate, quantities of interest, such as the diagonal elements of the pressure tensor and hence elongational viscosities, are then calculated by extrapolating their frequency-dependent values down to zero frequency. The main advantage of this technique is that it provides a convenient and consistent means of extrapolating to the zero-frequency (steady elongation) elongational viscosity, unlike the standard method, in which it may be difficult to distinguish between the transient response and the steady-state response. It may also be possible to extend this technique to the case of molecular fluids and thus extrapolate the steady-state zero-frequency viscoelastic properties of interest.

Another more obvious means of simulating steady elongational flow of molecular fluids is to apply a low strain rate to the system. As the maximum simulation time is inversely proportional to the elongational rate $\dot{\varepsilon}$ [6], it is clear that smaller values of $\dot{\varepsilon}$ will lead to longer simulation times. It is well known that direct NEMD is the most efficient strong-field method of calculating steady-state properties of interest, but is inefficient for small fields [7]. It was partly for this reason that Morriss and Evans [8–11,7] developed the technique of transient-time correlation functions (TTCFs) as an efficient method for extracting the transient response of a fluid under the influence of a weak external field. The TTCF technique has been successfully applied to planar shear simulations, with spectacular success. We will now apply the TTCF formalism to the case of steady elongational flow and will find similar efficiency at low strain rates.

II. THEORY

Using nonlinear isothermal response theory, Morriss and Evans [8] were able to demonstrate that for a fluid undergoing planar shear flow, any arbitrary phase variable $B(t)$ can be expressed in terms of a *nonequilibrium* transient time correlation function (TTCF)

$$\langle B(t)\rangle = \langle B(0)\rangle - \beta F_e \int_0^t ds \langle B(s)J(0)\rangle, \tag{1}$$

where $\beta = 1/kT$, k is Boltzmann's constant, and $J(0)$ is the dissipative flux at $t=0$, which is itself related to the adiabatic time derivative of the internal energy [8,9]. Here T is the temperature of the system that evolves from an equilibrium

configuration at $t=0$ to some final nonequilibrium state at time t and the angular brackets denote time averages. This derivation assumes that the applied field F_e is time independent, although recently Petravic and Evans [12] have extended this formalism to account for explicitly time-dependent fields. It is important to recognize that Eq. (1) represents the correlation of a nonequilibrium phase variable $B(t)$ at some time t, with an equilibrium ($t=0$) value of the dissipative flux. It represents the natural nonlinear generalization of the equilibrium Green-Kubo formulas. As $B(t)$ represents a general arbitrary phase variable, the task at hand involves identifying the appropriate values of the dissipative flux and external field for elongational flow.

For an atomic fluid undergoing planar shear flow, the adiabatic derivative of the internal energy H_0 is usually written as $\dot{H}_0=-JF_e$, where J and F_e are as previously defined. For more complex flows, one can generalize this to $\dot{H}_0=-\mathbf{J}:\mathbf{F}_e$, where now both $\mathbf{J}$ and $\mathbf{F}_e$ are tensorial quantities. For planar shear (or planar Couette) flow, it is easily seen that $\dot{H}_0=-\dot{\gamma}P_{xy}V$ [9], where $\dot{\gamma}$ is the strain rate, P_{xy} is the xy element of the pressure tensor (negative of the shear-stress), and V is the system volume.

For steady elongational flow without shear, we can write the applied strain rate tensor as

$$\nabla\mathbf{u}\equiv\mathbf{F}_e=\begin{pmatrix}\dot{\varepsilon}_{xx} & 0 & 0\\ 0 & \dot{\varepsilon}_{yy} & 0\\ 0 & 0 & \dot{\varepsilon}_{zz}\end{pmatrix}, \tag{2}$$

where $\mathbf{u}$ is the streaming velocity of the fluid. Assuming pairwise additive potential interactions between atoms, we can write the total internal energy of a particle as

$$H_i=\frac{\mathbf{p}_i^2}{2m_i}+\frac{1}{2}\sum_j \phi_{ij}, \tag{3}$$

where we note that the momenta $\mathbf{p}_i$ are peculiar with respect to $\mathbf{u}$. The total internal energy is thus $H_0=\Sigma_i H_i$. Assuming unthermostated SLLOD equations of motion for the particle dynamics [7],

$$\dot{\mathbf{r}}_i=\frac{\mathbf{p}_i}{m_i}+r_i\cdot\nabla\mathbf{u},$$

$$\dot{\mathbf{p}}_i=\mathbf{F}_i-\mathbf{p}_i\cdot\nabla\mathbf{u}, \tag{4}$$

it is straightforward to show that the adiabatic time derivative of the total internal energy is given by

$$\begin{aligned}\dot{H}_0&=-\dot{\varepsilon}_{xx}\sum_i\left[\frac{p_{xi}^2}{m_i}+F_{xi}x_i\right]-\dot{\varepsilon}_{yy}\sum_i\left[\frac{p_{yi}^2}{m_i}+F_{yi}y_i\right]\\&\quad-\dot{\varepsilon}_{zz}\sum_i\left[\frac{p_{zi}^2}{m_i}+F_{zi}z_i\right]\\&=-[\dot{\varepsilon}_{xx}P_{xx}+\dot{\varepsilon}_{yy}P_{yy}+\dot{\varepsilon}_{zz}P_{zz}]V=-[V\mathbf{P}:\nabla\mathbf{u}]\equiv-\mathbf{J}:\mathbf{F}_e.\end{aligned} \tag{5}$$

Following the procedure of Morriss and Evans [8], one can show that the time-dependent Gaussian isokinetic distribution function takes on the general form

$$\begin{aligned}f(\mathbf{\Gamma},t)&=\exp\left\{-\beta\int_0^t ds[\mathbf{J}(\mathbf{\Gamma},-s):\mathbf{F}_e]\right\}f(\mathbf{\Gamma},0)\\&=\exp\left\{-\beta\sum_{\delta,\sigma}F_{e_{\delta\sigma}}\left[\int_0^t ds\ J_{\sigma\delta}(\mathbf{\Gamma},-s)\right]\right\}\\&\quad\times f(\mathbf{\Gamma},0),\end{aligned} \tag{6}$$

where $f(\mathbf{\Gamma},0)$ is the time-independent equilibrium isokinetic distribution function, given as [7]

$$f(\mathbf{\Gamma},0)=\frac{\exp[-\beta\phi(\mathbf{\Gamma})]\delta(K(\mathbf{\Gamma})-K_0)}{\int d\mathbf{\Gamma}\ \exp[-\beta\phi(\mathbf{\Gamma})]\delta(K(\mathbf{\Gamma})-K_0)}. \tag{7}$$

Here ϕ is the total potential energy of the system, K is the total kinetic energy, and K_0 is the kinetic energy at which the system is constrained. One can now calculate the ensemble average of the time evolution of any phase variable in the usual manner,

$$\begin{aligned}\langle B(t)\rangle&=\int d\mathbf{\Gamma}\ B(\mathbf{\Gamma})f(\mathbf{\Gamma},t)\\&=\int d\mathbf{\Gamma}\ B(\mathbf{\Gamma})\exp\left\{-\beta\sum_{\delta,\sigma}F_{e_{\delta\sigma}}\left[\int_0^t ds\ J_{\sigma\delta}(\mathbf{\Gamma},-s)\right]\right\}\\&\quad\times f(\mathbf{\Gamma},0).\end{aligned} \tag{8}$$

Taking the time derivative of Eq. (8) and making use of the identity $\langle X(t)Y\rangle=\langle XY(-t)\rangle$, we find

$$\begin{aligned}\frac{\partial}{\partial t}\langle B(t)\rangle&=\int d\mathbf{\Gamma}\ B(\mathbf{\Gamma})\left(-\beta\sum_{\delta,\sigma}F_{e_{\delta\sigma}}J_{\sigma\delta}(\mathbf{\Gamma},-t)\right)f(\mathbf{\Gamma},t)\\&=-\beta\sum_{\delta,\sigma}F_{e_{\delta\sigma}}\langle B(t)J_{\sigma\delta}(0)\rangle.\end{aligned} \tag{9}$$

Note here that $J_{\sigma\delta}(0)$ refers to equilibrium values of $J_{\sigma\delta}$ at $t=0$. Finally, integrating Eq. (9) with respect to time generates the general relation for the time evolution of B,

$$\langle B(t)\rangle=\langle B(0)\rangle-\beta\sum_{\delta,\sigma}F_{e_{\delta\sigma}}\int_0^t ds\langle B(s)J_{\sigma\delta}(0)\rangle. \tag{10}$$

For the specific case of steady elongational flow with no shear, we substitute the values of $F_{e_{\delta\sigma}}$ and $J_{\sigma\delta}(0)$, derived in Eq. (5), into Eq. (10) and get

$$\begin{aligned}\langle B(t)\rangle&=\langle B(0)\rangle-\beta V\left[\dot{\varepsilon}_{xx}\int_0^t ds\langle B(s)P_{xx}(0)\rangle\right.\\&\quad+\dot{\varepsilon}_{yy}\int_0^t ds\langle B(s)P_{yy}(0)\rangle\\&\quad\left.+\dot{\varepsilon}_{zz}\int_0^t ds\langle B(s)P_{zz}(0)\rangle\right].\end{aligned} \tag{11}$$

For the purposes of this paper we are primarily concerned with calculating the diagonal elements of the pressure tensor $P_{\delta\delta}$, so we simply replace B with $P_{\delta\delta}$. We further note that Eq. (11) is valid for an isothermal system that evolves under the application of a Gaussian thermostat to the equations of

motion. This assumption is implicit in the derivation of the Gaussian isokinetic distribution function (6).

III. SIMULATIONS

The thermostated SLLOD equations of motion [7] that are used in this work are

$$\dot{\mathbf{r}}_i = \frac{\mathbf{p}_i}{m_i} + \mathbf{r}_i \cdot \nabla \mathbf{u},$$
$$\dot{\mathbf{p}}_i = \mathbf{F}_i - \mathbf{p}_i \cdot \nabla \mathbf{u} - \alpha \mathbf{p}_i, \tag{12}$$

where α is a Gaussian thermostat multiplier used to constrain the system to constant temperature, given as

$$\alpha = \frac{\Sigma_i \mathbf{p}_i \cdot [\mathbf{F}_i - (\mathbf{p}_i \cdot \nabla \mathbf{u})]}{\Sigma_i \mathbf{p}_i^2}. \tag{13}$$

Because elongational flow will involve a change in shape of the simulation cell, the periodic boundary conditions will evolve in time such that the lengths of either all or some of the simulation cell dimensions will decrease or increase with time. A simple integration of the equations of motion shows that the dimensions of the simulation cell change exponentially,

$$L_\delta(t) = L_\delta(0) \exp(\dot{\varepsilon}_{\delta\delta} t), \tag{14}$$

where $L_\delta(t)$ is the length of the simulation cell at time t in the direction δ ($\delta = x,y,z$).

If the flow is such that the system volume is a constant of the motion, then the dimensions must change in such a way that $\mathrm{Tr}(\nabla \mathbf{u}) = 0$. Thus the simulation will last only up to a specific time, at which the length of the cell in the contracting dimension reaches its minimum, i.e., $L_\delta(t_{\max}) = 2r_c$, where r_c is the cutoff radius for the potential interaction. This maximum time can be shown to be

$$t_{\max} = \dot{\varepsilon}_{\sigma\sigma}^{-1} \ln\left(\frac{2r_c}{L_\sigma(0)}\right), \tag{15}$$

where σ is the contracting dimension and $\dot{\varepsilon}_{\sigma\sigma}$ is negative.

Three kinds of elongational flow are considered in this paper: planar elongational flow (PEF), uniaxial stretching flow (USF), and biaxial stretching flow (BSF). PEF occurs when one of the diagonal elements in the strain rate tensor is zero and the other two are equal in magnitude and opposite in sign (stretching and compressing). USF implies that one element is positive (stretching) and the other two are negative (compressing) and of half the magnitude, while BSF implies that one element is negative (compressing) and the other two are positive (stretching) and of half the magnitude. These types of flow ensure that the system volume is a constant of the motion. For the geometry used in this work, PEF implies that $\dot{\varepsilon}_{xx} = -\dot{\varepsilon}$, $\dot{\varepsilon}_{yy} = \dot{\varepsilon}$, and $\dot{\varepsilon}_{zz} = 0$; USF implies that $\dot{\varepsilon}_{xx} = \dot{\varepsilon}$, $\dot{\varepsilon}_{yy} = -\frac{1}{2}\dot{\varepsilon}$, and $\dot{\varepsilon}_{zz} = -\frac{1}{2}\dot{\varepsilon}$; and BSF implies that $\dot{\varepsilon}_{xx} = -\dot{\varepsilon}$, $\dot{\varepsilon}_{yy} = \frac{1}{2}\dot{\varepsilon}$, and $\dot{\varepsilon}_{zz} = \frac{1}{2}\dot{\varepsilon}$.

The simulation cell consisted of $N = 108$ atoms that interact via the Weeks-Chandler-Andersen (WCA) potential [13] defined as $\phi(r) = 4(r^{-12} - r^{-6}) + 1$ for $r < 2^{1/6}$ and $\phi(r) = 0$ for $r > 2^{1/6}$, where we define the WCA potential constants σ and ε, as well as the mass of the atoms and Boltzmann's constant, to be unity for simplicity. Thus all measured properties are in dimensionless reduced units. The system is three dimensional and is periodic in all dimensions. All simulations are performed at the Lennard-Jones triple point $\rho = 0.8442$ and $T = 0.722$. The equations of motion were integrated using a fourth-order Runge-Kutta scheme and the integration time step was 0.001 in reduced units for all simulations. It is essential to use a self-starting integrator, such as the Runge-Kutta scheme, for TTCF calculations rather than Gear predictor-corrector or leapfrog integrators. The latter are accurate only after an initial startup period and are therefore unsuitable for the calculation of transient responses [9,11].

In all simulations, an equilibrium trajectory was maintained at a constant state point of $(\rho, T) = (0.8442,\ 0.722)$, while at equal intervals of 5000 time steps, two or three nonequilibrium trajectories were initiated (see below). This time separation was chosen to ensure that contiguous nonequilibrium trajectories were uncorrelated. The size of the equilibrium cell was $L_x = L_y = L_z = (N/\rho)^{1/3} = 5.0388$ and the nonequilibrium cell evolves such that L_x, L_y, and L_z vary with time according to Eq. (14) [6].

Morriss and Evans [9] demonstrated that for planar shear simulations, a substantial improvement in the signal-to-noise ratio at long times can be obtained through prudent phase-space symmetry mappings. This is also true for the case of elongational flow. If mixing occurs in the limit as $t \to \infty$, then $\langle B(t) P_{\delta\delta}(0) \rangle \sim \langle B(t) \rangle \langle P_{\delta\delta}(0) \rangle$. In general, for a nonequilibrium phase variable, $\langle B(t) \rangle \neq 0$. Morriss and Evans [9] showed that for planar shear flow, if one could generate an ensemble of initial phases such that $\Sigma_i P_{xy}(\mathbf{\Gamma}_i(0)) = 0$, then as a consequence of mixing, the statistical uncertainties at long time that are associated with small nonzero fluctuations around $P_{xy}(0)$ will be eliminated. In the case of elongational flow, we require $\Sigma_i \Sigma_\delta \dot{\varepsilon}_{\delta\delta} P_{\delta\delta}(\mathbf{\Gamma}_i(0)) = 0$. An appropriate phase-space mapping that can achieve this for our PEF simulations is $\mathbf{\Gamma}_1 \to \mathbf{\Gamma}_2$, where $\mathbf{\Gamma}_1 = (x_i, y_i, z_i, p_{xi}, p_{yi}, p_{zi})$ and $\mathbf{\Gamma}_2 = (y_i, x_i, z_i, p_{yi}, p_{xi}, p_{zi})$. Thus $P_{xx}(\mathbf{\Gamma}_2(0)) = P_{yy}(\mathbf{\Gamma}_1(0))$ and $P_{yy}(\mathbf{\Gamma}_2(0)) = P_{xx}(\mathbf{\Gamma}_1(0))$. This mapping has the necessary requirements that it preserves the total internal energy of the equilibrium system at $t = 0$, while ensuring at the same time that the new nonequilibrium trajectory ($\mathbf{\Gamma}_2$) evolves along a distinct path to the original nonequilibrium trajectory ($\mathbf{\Gamma}_1$). $\mathbf{\Gamma}_2$ is not a unique mapping scheme and other appropriate schemes are possible. For USF and BSF two initial equilibrium phases are insufficient for zeroing the long-time fluctuations. Now we require an additional phase-space mapping $\mathbf{\Gamma}_1 \to \mathbf{\Gamma}_3$, where $\mathbf{\Gamma}_3 = (z_i, y_i, x_i, p_{zi}, p_{yi}, p_{xi})$. Once again, this is not a unique mapping.

IV. RESULTS AND DISCUSSION

In Fig. 1 the results of direct and TTCF calculations of the diagonal elements of the pressure tensor are displayed for a PEF simulation with $\dot{\varepsilon}_{xx} = -0.5$, $\dot{\varepsilon}_{yy} = 0.5$, and $\dot{\varepsilon}_{zz} = 0$. The simulation consists of a total of $20 \times 2 \times 1185$ nonequilibrium trajectories, each 1100 time steps in duration (a total of 1.1 time units per nonequilibrium trajectory). It is clear that for this relatively moderate value of applied elongational rate, the direct results are statistically superior to those of the

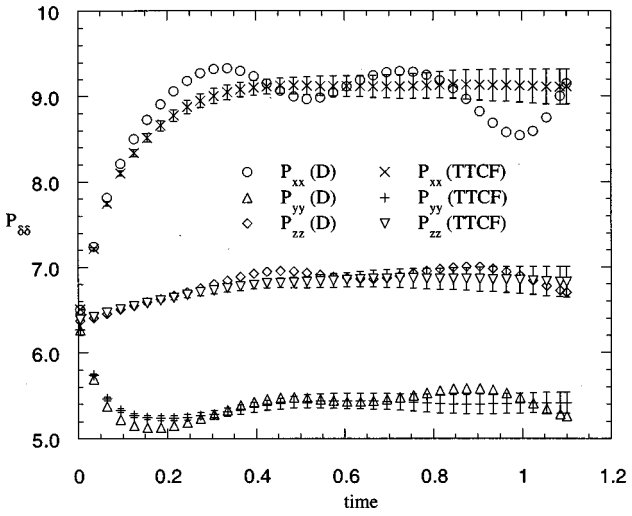

FIG. 1. Direct (D) and TTCF calculations of the diagonal elements of the pressure tensor for a PEF simulation with an applied strain rate of $\dot{\varepsilon}_{xx}=-0.5$, $\dot{\varepsilon}_{yy}=0.5$, and $\dot{\varepsilon}_{zz}=0$. Error bars for direct pressures are smaller than the plotted symbols. All pressures are in reduced units and are dimensionless.

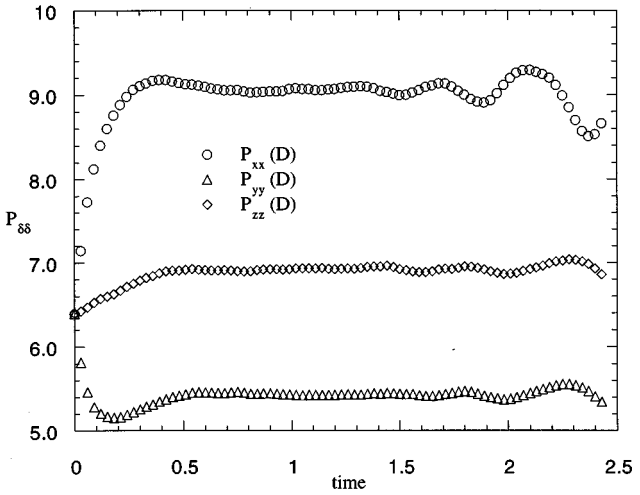

FIG. 2. Direct (D) pressures for the $N=864$ PEF system. The strain rate is the same as in Fig. 1.

TTCF method, which is to be expected [7].

As explained in a previous paper [6], the differences in the various elements of the pressure tensor can be explained in terms of the average spacing between atoms in any particular direction. We note that $P_{yy}<P_{zz}<P_{xx}$. This is to be expected, as the average spacing of atoms in the contracting x direction should be less than the average spacing of atoms in the stationary z direction, which in turn should be less than the average spacing of atoms in the expanding y direction. Thus the contribution to the configurational part of the pressure tensor will be greatest in the contracting direction and least in the expanding direction, as observed.

Interestingly, the direct results show significant oscillations in all elements of the pressure tensor, but are greatest for the pressure that corresponds to that measured in the contracting dimension (i.e., P_{xx}). These oscillations are possibly a consequence of shock waves or sound waves propagating through the fluid as a result of the application of a stepwise discontinuous strain rate at $t=0$. To check this, a simulation of $N=864$ atoms was performed at the same temperature, density, and strain rate. In this case all initial box lengths are exactly twice those of the $N=108$ simulations. This allows for a simulation of ~ 2.2 times as long [see Eq. (15)]. Direct averages of the pressures were taken over 400 NEMD trajectories. As seen in Fig. 2, the oscillations now appear at later times. If t_1 corresponds to the time at which a peak or trough occurs in the $N=108$ system and t_2 to corresponding times in the $N=864$ system, one can show from Eq. (14) that $t_2-t_1=\Delta$, where $\Delta=-(1/|\dot{\varepsilon}_{\delta\delta}|)\ln(\frac{1}{2})$. This assumes that waves propagate through both systems at a constant velocity. Thus $t_2=1.386+t_1$. From Figs. 1 and 2 this does indeed appear to be the case. If the system is large enough and the simulation could be run for longer times, presumably these oscillations would damp out at later times, leaving only constant values for the steady-state pressures.

The TTCF results in Fig. 1 demonstrate no measurable oscillations in any of the elements of the pressure tensor. This is particularly clear in the P_{xx} data, where the magnitude of the oscillations in the direct P_{xx} are sufficiently large to stand out against the statistical errors in the TTCF results. TTCF tends to wash out these oscillations and predicts only the long-time steady-state value of the pressure in any direction. This can be particularly useful if one is only interested in the long-time steady-state response of a fluid to an applied strain rate, as indeed is the case in the atomistic simulation of elongational flow. Of significant interest in such simulations is the extraction of the elongational viscosity, which is related to the steady-state value of the diagonal elements of the pressure tensor [1–6]. In such cases, spurious oscillations in the pressure actually tend to mask the genuine long-time steady-state value of the viscosity and increase its statistical uncertainty. The use of TTCF now provides a reliable and powerful means of removing any ambiguity between the transient response of a fluid to an applied field and its true steady-state response.

In Fig. 3 the results of a BSF simulation with $\dot{\varepsilon}_{xx}=-0.5$, $\dot{\varepsilon}_{yy}=0.25$, and $\dot{\varepsilon}_{zz}=0.25$, consisting of $10\times3\times1000$ NEMD trajectories, is shown. Once again we notice oscillations in the direct pressures, but none in the TTCF results. The values of P_{yy} and P_{zz} are identical to within statistical uncertainties, which is to be expected, as the fluid expands at equal rates in these two dimensions. Similarly, in Fig. 4 the results of a USF simulation consisting of the same number of trajectories is displayed. In this case, $\dot{\varepsilon}_{xx}=0.5$, $\dot{\varepsilon}_{yy}=-0.25$, and $\dot{\varepsilon}_{zz}=-0.25$. We note now that the magnitudes of the oscillations are almost equal in the expanding x direction and the contracting y and z directions due primarily to the magnitude of the field in the former being twice as large as that in the latter two. For equal field magnitudes, such as for PEF, oscillations are more pronounced in the contracting direction. Clearly the magnitude of these oscillations depends not just on the magnitude of the field in any particular direction, but also on whether the fluid is expanding or contracting in this direction. However, the TTCF results once again display no discernible oscillations, making the method ideally suited for studying the long-time steady-state behavior of fluids under a variety of different flow situations.

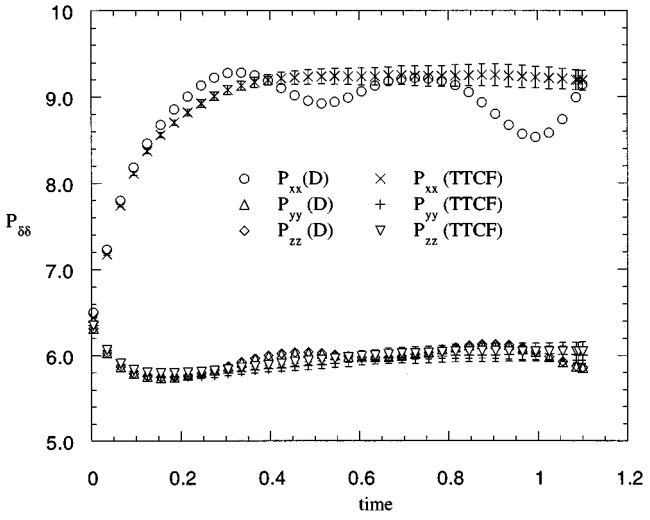

FIG. 3. Direct (D) and TTCF pressures for a BSF simulation with an applied strain rate of $\dot{\varepsilon}_{xx}=-0.5$, $\dot{\varepsilon}_{yy}=0.25$, and $\dot{\varepsilon}_{zz}=0.25$. Error bars for direct pressures are smaller than the plotted symbols.

Figure 5 shows direct and TTCF pressures for a PEF simulation with an applied strain rate of $\dot{\varepsilon}_{xx}=-0.001$, $\dot{\varepsilon}_{yy}=0.001$, and $\dot{\varepsilon}_{zz}=0$. This simulation consisted of a total of $10\times2\times5000$ NEMD trajectories, each of 1.1 time units in duration. We note here that the total available simulation time for this weak flow is ~550 time units. However, because of the low value of the elongational strain rate, the fluid attains a steady state in only a fraction of this total available time, allowing for a substantially shorter run time. In this weak flow regime TTCF is manifestly more efficient than the direct method, with errors in the TTCF calculations some 5–10 times smaller than corresponding errors in the direct pressures.

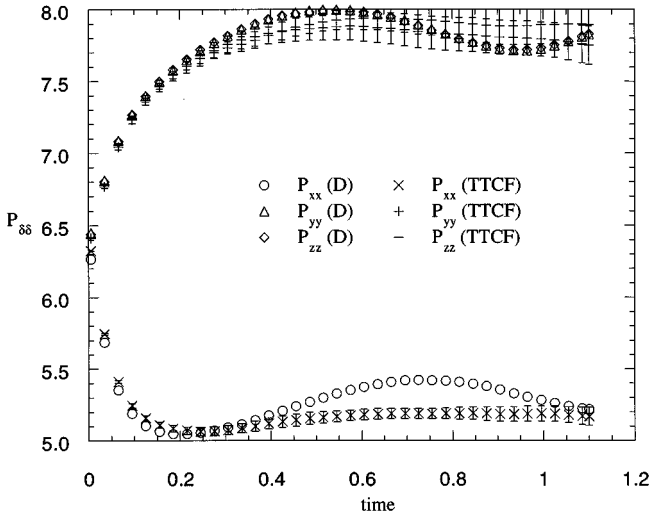

FIG. 4. Direct (D) and TTCF pressures for a USF simulation with an applied strain rate of $\dot{\varepsilon}_{xx}=0.5$, $\dot{\varepsilon}_{yy}=-0.25$, and $\dot{\varepsilon}_{zz}=-0.25$. Error bars for direct pressures are smaller than the plotted symbols.

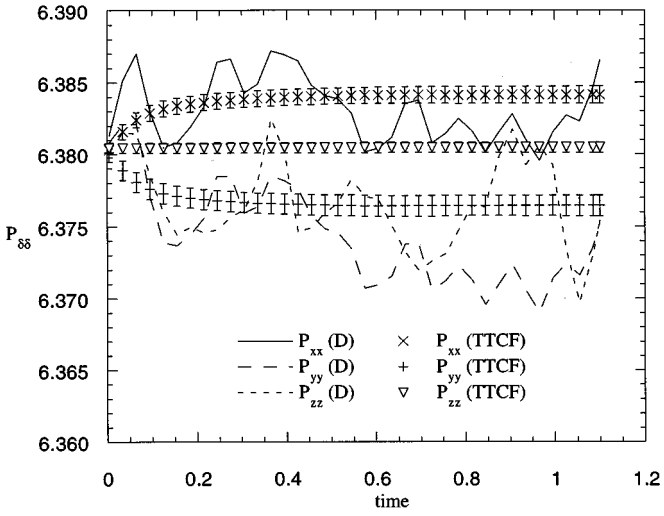

FIG. 5. Direct (D) and TTCF calculations of the diagonal elements of the pressure tensor for a PEF simulation with an applied strain rate of $\dot{\varepsilon}_{xx}=-0.001$, $\dot{\varepsilon}_{yy}=0.001$, and $\dot{\varepsilon}_{zz}=0$. Error bars for direct pressures (not shown) are $\sim5-10$ times larger than corresponding TTCF error bars.

Finally, it is important to note that all the above results were generated by incorporating the phase-space mapping scheme described in Sec. III above. Simulations were also conducted on systems without the application of phase-space mapping and the statistical errors in the TTCF results were seen to be at least an order of magnitude worse than those achieved with phase-space mapping. It is thus essential that any TTCF calculations incorporate an appropriate mapping scheme to achieve satisfactory numerical efficiency.

V. CONCLUSION

It has been demonstrated that the transient-time correlation function technique of Morriss and Evans [8–11,7] can be successfully applied to a simple atomic fluid undergoing steady elongational flow. The TTCF method demonstrates spectacular success at low elongational strain rates, where direct nonequilibrium time-averaged phase variables suffer from intolerable statistical noise. TTCF is also valid for higher elongational strain rates, but is seen to be less efficient than direct averaging. TTCF fails to account for real oscillations in the pressure at higher strain rates that are possibly a consequence of the propagation of shock waves or sound waves that result from the response of the fluid to an initial stepwise discontinuous perturbing field. However, despite this limitation it does, more importantly, correctly predict the long-time steady-state pressures that are required to calculate steady-state elongational viscosities. This filtering property of the TTCF method is actually highly desirable and ideally suited for this purpose.

Since TTCF for elongational flow achieves such excellent success for low elongational strain rates, it is hoped that this technique can be successfully applied to the NEMD simula-

tion of more complex molecular fluids. Such fluids require long simulation times in order to reach a steady state, and simulations with low applied strain rates may have the desirable property that the relaxation time of the fluid is sufficiently smaller than the total simulation time. It remains to be seen whether such fluids under the influence of these relatively low, but physically more reasonable, applied strain rates would demonstrate significant non-Newtonian behavior.

ACKNOWLEDGMENTS

The author wishes to thank Professor Denis Evans and Dr. Peter Daivis for useful discussions related to this work.

[1] D. M. Heyes, Chem. Phys. **98**, 15 (1985).
[2] M. W. Evans and D. M. Heyes, Mol. Phys. **69**, 241 (1990).
[3] J.-P. Ryckaert, Ber. Bunsenges. Phys. Chem. **94**, 256 (1990).
[4] M. N. Hounkonnou, C. Pierleoni, and J.-P. Ryckaert, J. Chem. Phys. **97**, 9335 (1992).
[5] A. Baranyai and P. T. Cummings, J. Chem. Phys. **103**, 10 217 (1995).
[6] B. D. Todd and P. J. Daivis, J. Chem. Phys. **107**, 1617 (1997).
[7] D. J. Evans and G. P. Morriss, *Statistical Mechanics of Non-equilibrium Liquids* (Academic, London, 1990).
[8] G. P. Morriss and D. J. Evans, Mol. Phys. **54**, 629 (1985).
[9] G. P. Morriss and D. J. Evans, Phys. Rev. A **35**, 792 (1987).
[10] D. J. Evans and G. P. Morriss, Mol. Phys. **61**, 1151 (1987).
[11] D. J. Evans and G. P. Morriss, Phys. Rev. A **38**, 4142 (1988).
[12] J. Petravic and D. J. Evans, Phys. Rev. Lett. **78**, 1199 (1997).
[13] J. D. Weeks, D. Chandler, and H. C. Andersen, J. Chem. Phys. **54**, 5237 (1971).